UPGRADES TO THE DARHT SECOND AXIS INDUCTION CELLS

K. Nielsen[ξ], J. Barraza, M. Kang, F. Bieniosek[†], K. Chow[†], W. Fawley[†], E. Henestroza[†], L. Reginato[†], W. Waldron[†], B. Prichard[+], Richard J. Briggs[‡], T. Genoni[#], T. Hughes

Los Alamos National Laboratory, PO Box 1663, Mail Stop P942
Los Alamos, New Mexico, US

Abstract

The Dual-Axis Radiographic Hydrodynamics Test (DARHT) facility will employ two perpendicular electron Linear Induction Accelerators to produce intense, bremsstrahlung x-ray pulses for flash radiography. The second axis, DARHT II [1], features a 3-MeV, 2-kA injector and a 15-MeV, 1.6-microsecond accelerator consisting of 74 induction cells and drivers. Major induction cell components include high flux swing magnetic material (Metglas 2605SC) and a Mycalex™ insulator. The cell drivers are pulse forming networks (PFNs). The DARHT II accelerator cells have undergone a series of test and modeling efforts to fully understand their operational parameters. These R&D efforts have identified problems in the original cell design and means to upgrade the design, performance and reliability of the linear induction cells. Physical changes in the cell oil region, the cell vacuum region, and the cell drivers, together with different operational and maintenance procedures, have been implemented in the prototype units resulting in greatly enhanced cell performance and reliability. A series of prototype acceptance tests have demonstrated that the required cell reliability and lifetime is exceeded at the increased performance levels. Shortcomings of the original design are summarized and improvements to the design, their resultant enhancement in performance, and various test results are discussed.

I. Introduction

DARHT II accelerator cells were originally outfitted with voltage monitors that were later found to be non-linear, resulting in the cells being tested at ~18% below the specified 193 kV. After monitors were replaced and voltage levels corrected, performance shortcomings were discovered in both the oil and vacuum regions of the cells.

In the vacuum region both insulator flashover and cathode to anode breakdown were observed. Vacuum breakdown included faults during the accelerating pulse and faults after the accelerating pulse during reversal.

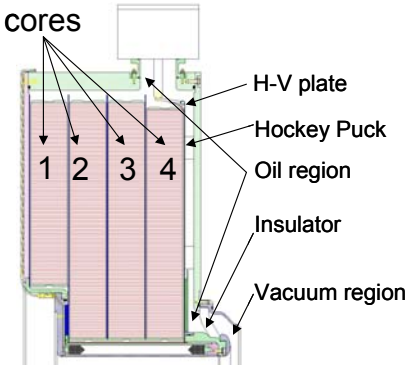

Figure 1. Cross-section of the original DARHT II induction cell design.

II. Cell Oil Region

In the oil region most high voltage breakdowns occurred on the outer edge of the cores, in the upper quadrant of the cells, and the majority of the damage was between core 4 and the high voltage plate, or between cores 3 and 4. Some standoffs, or hockey pucks, between the high voltage plate and end plate also tracked. In order to test the cell oil region the vacuum region of the cell was filled with oil. In addition, modeling efforts were undertaken to better understand field distributions in the cell oil region. The results of calculations and early experiments with cell modification led to the global modification of cell electric fields by extending the cell length.

A. Modification of Cell Oil Region Details

The original solid insulation between cores consisted of multiple layers of Mylar. The ~ 70-inch diameter cores were wound from 0.8 mil Metglas tape insulated with a layer of 0.2-mil Mylar. The Mylar layer extends ~0.05 inches on each side beyond the width of the 4-inch wide Metglas. A core contains ~ 20,000 turns of the Metglas with each turn separated by a layer of Mylar. The layers of 0.2-mil Mylar contact the Mylar sheets that separate the cores. This area and the region between core-

* This work was supported by the US National Nuclear Security Agency and the US Department of Energy under contract W-7405-ENG-36
ξ email: knielsen@lanl.gov
† *LBNL, Berkeley, CA 94720 USA*
+ *SAIC, Los Alamos, NM 87544 USA*
‡ *SAIC, Alamo, CA 94507 USA*
# *ATK-MR, Albuquerque, NM 87110 USA*

Report Documentation Page

Form Approved
OMB No. 0704-0188

1. REPORT DATE	2. REPORT TYPE	3. DATES COVERED
JUN 2005	**N/A**	**-**

4. TITLE AND SUBTITLE	5a. CONTRACT NUMBER
Upgrades To The Darht Second Axis Induction Cells	5b. GRANT NUMBER
	5c. PROGRAM ELEMENT NUMBER
6. AUTHOR(S)	5d. PROJECT NUMBER
	5e. TASK NUMBER
	5f. WORK UNIT NUMBER
7. PERFORMING ORGANIZATION NAME(S) AND ADDRESS(ES) **Los Alamos National Laboratory, PO Box 1663, Mail Stop P942 Los Alamos, New Mexico, US**	8. PERFORMING ORGANIZATION REPORT NUMBER
9. SPONSORING/MONITORING AGENCY NAME(S) AND ADDRESS(ES)	10. SPONSOR/MONITOR'S ACRONYM(S)
	11. SPONSOR/MONITOR'S REPORT NUMBER(S)

12. DISTRIBUTION/AVAILABILITY STATEMENT

Approved for public release, distribution unlimited

13. SUPPLEMENTARY NOTES

See also ADM002371. 2013 IEEE Pulsed Power Conference, Digest of Technical Papers 1976-2013, and Abstracts of the 2013 IEEE International Conference on Plasma Science. IEEE International Pulsed Power Conference (19th). Held in San Francisco, CA on 16-21 June 2013., The original document contains color images.

14. ABSTRACT

The Dual-Axis Radiographic Hydrodynamics Test (DARHT) facility will employ two perpendicular electron Linear Induction Accelerators to produce intense, bremsstrahlung x-ray pulses for flash radiography. The second axis, DARHT II [1], features a 3-MeV, 2-kA injector and a 15-MeV, 1.6-microsecond accelerator consisting of 74 induction cells and drivers. Major induction cell components include high flux swing magnetic material (Metglas 2605SC) and a MycalexTM insulator. The cell drivers are pulse forming networks (PFNs). The DARHT II accelerator cells have undergone a series of test and modeling efforts to fully understand their operational parameters. These R&D efforts have identified problems in the original cell design and means to upgrade the design, performance and reliability of the linear induction cells. Physical changes in the cell oil region, the cell vacuum region, and the cell drivers, together with different operational and maintenance procedures, have been implemented in the prototype units resulting in greatly enhanced cell performance and reliability. A series of prototype acceptance tests have demonstrated that the required cell reliability and lifetime is exceeded at the increased performance levels. Shortcomings of the original design are summarized and improvements to the design, their resultant enhancement in performance, and various test results are discussed.

15. SUBJECT TERMS

16. SECURITY CLASSIFICATION OF:			17. LIMITATION OF ABSTRACT	18. NUMBER OF PAGES	19a. NAME OF RESPONSIBLE PERSON
a. REPORT **unclassified**	b. ABSTRACT **unclassified**	c. THIS PAGE **unclassified**	**SAR**	**4**	

Standard Form 298 (Rev. 8-98)
Prescribed by ANSI Std Z39-18

separating Mylar sheets created air bubble traps in the oil region.

Additionally, the layers of Metglas have a tendency to telescope and create enhanced local fields. The edges of stainless steel bands along the outer edge of the cores were also a source of enhanced local fields. Extensive efforts were undertaken to reduce the likelihood of air bubbles in the oil and reduce enhanced local fields. The multiple Mylar sheets were replaced with a single 63-mil thick sheet of high-density polyethylene. In addition, 8 radial poly slats were used between the cores and poly sheets to improve oil circulation and prevent trapped air. Efforts were made to reduce core telescoping, and corner radii were increased and polished. These efforts improved the cell performance but were found to be inadequate to reliably meet specifications.

.

B. Cell Oil Region Extension

Four modeling efforts were undertaken to understand electric field distribution within the oil region of the cell. The four include a time dependent electromagnetic model [2], an analytical model [3], an electrostatic model, and a capacitive ladder circuit model. All of these models reinforced each other and revealed higher than expected electric fields between the outer edge of core 4 and the high voltage plate, and between core 4 and core 3. Figure 2 shows results from the electromagnetic model. These calculations showed that the core-to-core capacitance was much smaller than expected, and the core-to-housing stray capacitance was comparable to the core-to-core capacitance, resulting in an uneven voltage distribution between cores. The reason for the lower than expected core-to-core capacitance is that the radial Metglas layer-to-layer capacitance and the axial core-to-core capacitance constitute a capacitive ladder line. The result is an effective core-to-core capacitance involving only an inch or so of the outer edge of the core face where the potential difference to the adjacent core is highest.

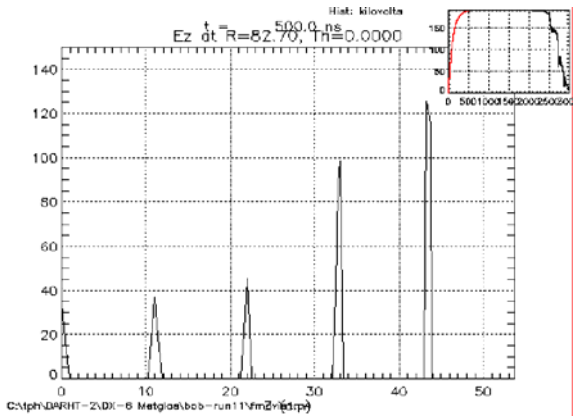

Figure 2: Calculation of the Electric Fields at the outer edge of the cores as a function of axial position. The highest field ~125 kV/cm occurs between core 4 and the high voltage plate.

The stray capacitance from core-to-housing pulled down the potential on the outer edge of the cores and resulted in a very high potential difference between the high voltage plate and the outer edge of core 4, and between the outer edge of core 4 and the outer edge of core 3. Extending the gap between core 4 and the high voltage plate reduced the fields in this region to roughly the levels experienced between each core.

Increasing the distance between core 4 and the high voltage plate from the original 0.25 inches to 1.0 inch reduced the calculated peak fields by nearly a factor of 4 and also reduced the other core-to-core fields by a substantial factor. These calculations were verified in a small-scale test where core-to-core potentials could be measured directly. Figure 3 shows the resultant fields with and without extension measured on the small-scale test.

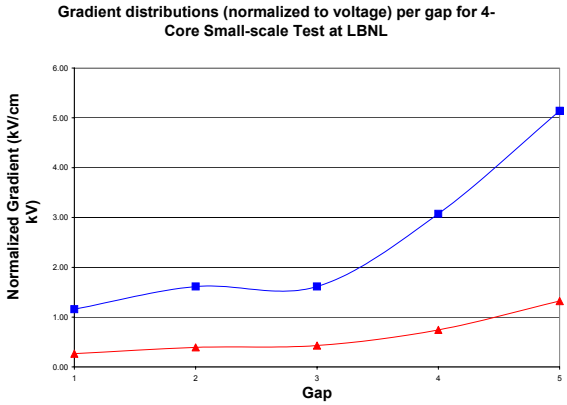

Figure 3: Normalized gradient (kV/cm-kV) measured in a small-scale mock-up of the cell. The upper trace is without extension and the lower trace demonstrates field reduction due to extension.

C. Hockey Puck Extension

The extension of the cell provided ample room to increase the length of the high voltage plate to endplate standoffs or hockey pucks. Recesses were stamped in the high voltage plate and pockets were machined in the end plate, which increased the hockey puck length from 1.0 inch to 1.5 inches. A cross section of the cell is shown in Figure 4, where the recesses that allow hockey puck extension and reduce the fields at the end of the pucks are shown.

Figure 4 shows the cell housing length increased by the addition of a 1-inch thick ring on the outer diameter and the addition of a 1-inch thick ring on the inner diameter [4]. To fill up the additional length in the oil volume, 1-inch poly-spoke spacers are placed between core 4 and the high voltage plate.

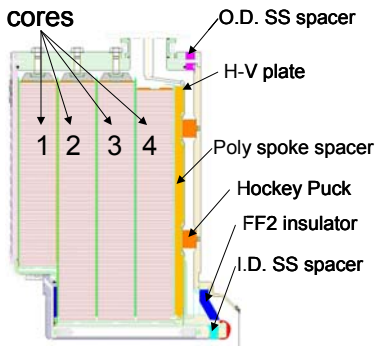

Figure 4: A cross-section of the upper oil region of the extended cell.

III. Cell Vacuum Region

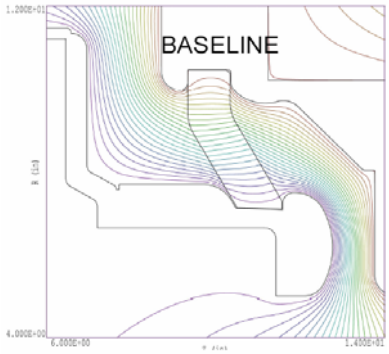

Figure 5: The calculated equal potential lines for the original baseline vacuum insulator design.

Electrostatic calculations were undertaken to examine the field distribution along the insulator and in the accelerating gap. A finer mesh size than used in the original design effort revealed more field peaking in the anode triple point region and the cathode triple point region than previously reported [5]. At the cathode end, the field lines were angled such that electrons leaving some portions of the cathode could intersect the insulator and avalanche leading to insulator flashover.

A. Flatface 1

FF1 was a modification of the original insulator design and featured a continuous flat profile from the anode to the cathode. FF1 had a large gap between the insulator and anode shield, which reduced the field peaking in the anode triple point region, and a revised cathode triple point region that reduced fields and corrected field angles to carry electrons away from the insulator. A cross-section of FF1 with its calculated equal potential lines is shown in Figure 6.

When tested on the Insulator Test Stand (ITS) at LBNL, FF1 was pulsed at increasing voltages up to the limit of the test stand (340 kV) and operated there for over a thousand pulses with no failures. The problem with the FF1 design is that the reduction of cross-section in the anode region reduced its mechanical strength, making it unsatisfactory for use on a cell.

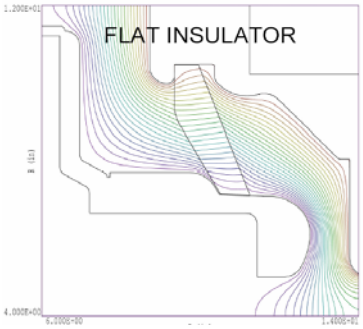

Figure 6: A calculation of the equal potential lines for Flatface 1 (FF1)

B. Flatface 2

Flatface 2 (FF2) was originally tested to determine whether the cathode region modifications of FF1 would improve the original design without the mechanical strength reductions incorporated into the anode region of FF1. Figure 7 shows a cross section of the FF2 design and calculated equal potential lines. Figures 8 & 9 show the reduction in the peak electrical field near the cathode and the reversal of field angles from negative to positive values. The figures also demonstrate the similarity of FF1 (Flat Insulator) and FF2 (New Design) at the cathode end.

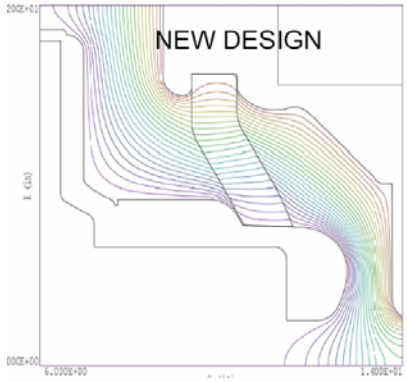

Figure 7: Calculated equal potential lines for FF2

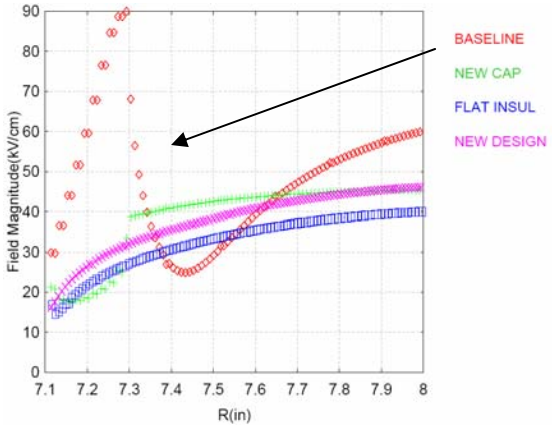

Figure 8: Reduction in electric field peaking along insulator surface near the cathode triple point.

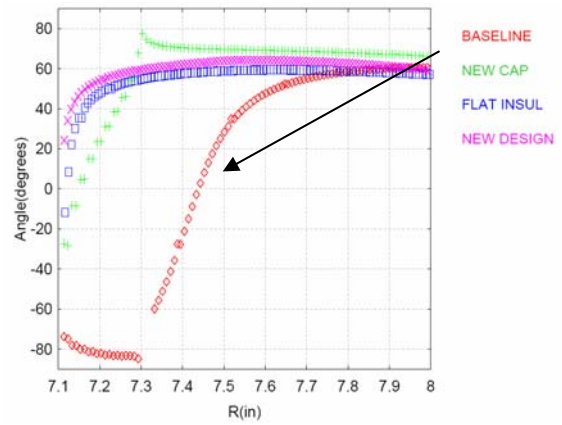

Figure 9: A comparison of field angles along insulator surface showing proper angles near the cathode.

The FF2 performed as well on the ITS as FF1. It was tested up to 340 kV for over a thousand ≤3 microsecond pulses without any breakdowns

C. Diode Boards

The design of FF2 does not address the peaking of the field at the anode triple point region. This becomes an issue during the reversal when the anode effectively becomes the cathode. Since vacuum breakdowns had been frequently observed during reversal, the anode region had to be addressed. This was accomplished by clamping the reversal of the cell with a diode string mounted in the PFN. Reversal with the original PFN design was >80%. Figure 10 shows the minimal reversal with the diode reversal clamping string in the PFN. Reversal occurs due to saturation of the Metglas cores late in the pulse.

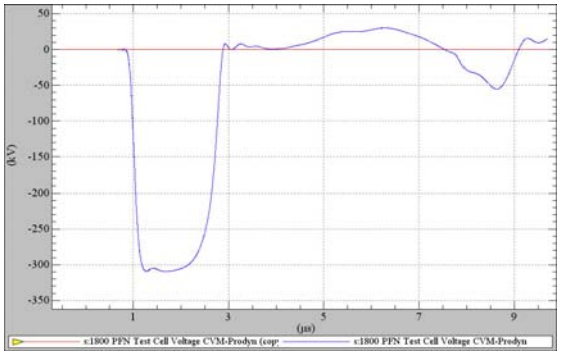

Figure 10: The voltage waveform for a 300 kV pulse showing a reversal of less than 40 kV or ~13% using a PFN with reversal clamping diodes.

Using the diode string to eliminate reversal removed problems created by the anode region field peaking. This eliminated the need to modifiy the anode end of the insulator and made FF2 a viable solution to the vacuum insulator problem.

IV. Acceptance Testing

Successful modification of the oil region utilizing the extended cell, and modification of the vacuum region utilizing FF2 led to integrated testing of the entire cell. An extended cell with FF2 was first assembled as a pre-prototype (PP-1) at LANL and tested for 15,200 pulses at 300 kV without any failures. Similar success was experienced at LBNL as part of the insulator testing. These successes led to the establishment of a new baseline design for the DARHT II Refurbishment and Commissioning project. To demonstrate the reliability of the new baseline, an acceptance-testing program was established that would statistically demonstrate the required reliability.

The acceptance tests allowed for a maximum of 8 faults to occur during the testing sequence. The acceptance testing has been completed, and no faults have occurred. In fact, the testing exceeded the required number of pulses on each of units 4 by over 3000 pulses. Over 200,000 test pulses at voltages ≥ 200 kV and over 70,000 pulses at voltages >250 kV were fired with no failures.

The acceptance test sequence has demonstrated that the new cell baseline for the DARHT II refurbishment project exceeds its required specifications.

V. Conclusion

The original DARHT II accelerator cells' design experienced shortcomings in both the oil and vacuum regions. The problems in the oil region have been solved by extending the cells, extending the hockey pucks, increasing the spacing between core 4 and the high voltage plate, and attention to detail to eliminate air bubbles and field enhancements. Modifying the vacuum insulator to a FF2 geometry and clamping reversal with diode strings in the PFN have addressed the vacuum region problems.

Statistically significant acceptance testing of the revised cell baseline design has demonstrated that the new design exceeds its required specifications. This revised cell design is the basis of the DARHT II Refurbishment and Commissioning project.

VI. References

[1] Burns, M. J. et. al., "Status of the DARHT Phase 2 Long-Pulse Accelerator," PAC2001, Chicago, IL, June 2001, p.325

[2] Hughes, T. P. et. al., "Numerical Model of the DARHT Accelerating Cell," poster FPAT033, this meeting.

[3] Briggs, R. J, and Fawley, W. M., "A Simple Model for Induction Core Voltage Distributions, DARHT Technical Note No. 418, June 25, 2004

[4] Barraza, J. et. al., "Mechanical Engineering Upgrades to the DARHT-II Induction Cells," 15th IEEE Pulse Power Conference, Monterey, CA, June 2005

[5[Rutkowski, H. L. et.al., "A Long Pulse Linac for the Second Phase of DARHT" PAC1999, New York, p. 21